

Diffusion phenomena in a mixed phase space

Cite as: Chaos **30**, 013108 (2020); <https://doi.org/10.1063/1.5100607>

Submitted: 18 April 2019 . Accepted: 04 December 2019 . Published Online: 07 January 2020

Matheus S. Palmero , Gabriel I. Díaz, Peter V. E. McClintock, and Edson D. Leonel



View Online



Export Citation



CrossMark

ARTICLES YOU MAY BE INTERESTED IN

[Characterizing the complexity of time series networks of dynamical systems: A simplicial approach](#)

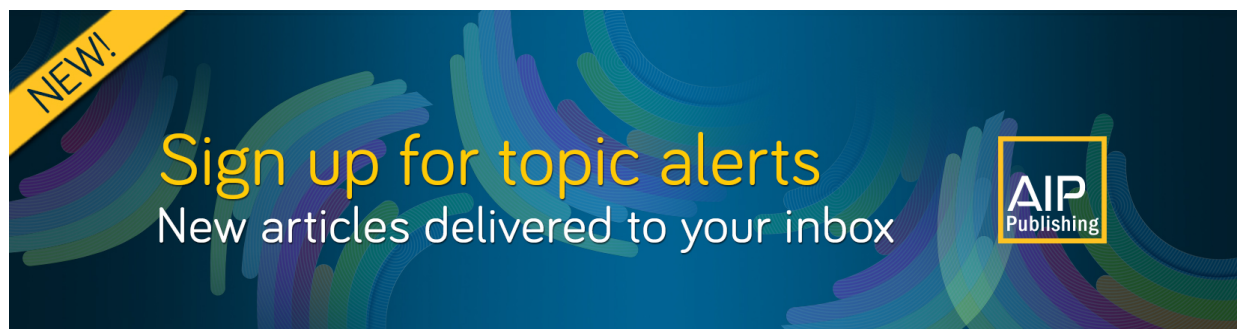
Chaos: An Interdisciplinary Journal of Nonlinear Science **30**, 013109 (2020); <https://doi.org/10.1063/1.5100362>

[Functionability in complex networks: Leading nodes for the transition from structural to functional networks through remote asynchronization](#)

Chaos: An Interdisciplinary Journal of Nonlinear Science **30**, 013105 (2020); <https://doi.org/10.1063/1.5099621>

[Using machine learning to predict extreme events in the Hénon map](#)

Chaos: An Interdisciplinary Journal of Nonlinear Science **30**, 013113 (2020); <https://doi.org/10.1063/1.5121844>



NEW!

Sign up for topic alerts

New articles delivered to your inbox

AIP
Publishing



Diffusion phenomena in a mixed phase space

Cite as: Chaos 30, 013108 (2020); doi: 10.1063/1.5100607

Submitted: 18 April 2019 · Accepted: 4 December 2019 ·

Published Online: 7 January 2020



View Online



Export Citation



CrossMark

Matheus S. Palmero,^{1,2,3}  Gabriel I. Díaz,³ Peter V. E. McClintock,² and Edson D. Leonel¹

AFFILIATIONS

¹Departamento de Física, UNESP—Univ Estadual Paulista, Av. 24A, 1515, Bela Vista, 13506-900 Rio Claro, SP, Brazil

²Department of Physics, Lancaster University, Lancaster LA1 4YW, United Kingdom

³Instituto de Física—Universidade de São Paulo (IFUSP), Rua do Matão, Tr.R 187, Cidade Universitária, 05314-970 São Paulo, SP, Brazil

ABSTRACT

We show that, in strongly chaotic dynamical systems, the average particle velocity can be calculated analytically by consideration of Brownian dynamics in a phase space, the method of images, and the use of the classical diffusion equation. The method is demonstrated on the simplified Fermi-Ulam accelerator model, which has a mixed phase space with chaotic seas, invariant tori, and Kolmogorov-Arnold-Moser islands. The calculated average velocities agree well with numerical simulations and with an earlier empirical theory.

© 2020 Author(s). All article content, except where otherwise noted, is licensed under a Creative Commons Attribution (CC BY) license (<http://creativecommons.org/licenses/by/4.0/>). <https://doi.org/10.1063/1.5100607>

We present a part-empirical, part-analytical approach to the analysis of diffusion in chaotic dynamical systems. It relies on the application of a fundamental idea from classical continuum physics (probabilistic diffusion) to chaotic systems that are, of course, inherently deterministic. In particular, we consider diffusion and Brownian dynamics in the phase space of a chaotic system and show how the diffusion equation, applied in this context, can provide an accurate description of the average velocity and its evolution, even when the model presents anomalous effects. To demonstrate and validate the formalism, we take a well-known example from astrophysics—the simplified Fermi-Ulam model.

I. INTRODUCTION

The evolution of systems described by Hamiltonians with nonlinear terms in their dynamical equations may exhibit either regularity or chaos. The result is often a mixed phase space containing chaotic seas, invariant tori, and Kolmogorov-Arnold-Moser (KAM) islands.¹ Dynamical systems with strong chaotic motion often exhibit diffusive behavior.^{2,3} An intuitive example of this is to drop colored ink into water, observing how the particles of ink move away from each other, spreading out into the liquid. For a mixed phase space, however, an initial condition, e.g., around a KAM island may lead to very complicated behavior. The stability structures influence directly the transport properties of chaotic orbits,⁴ often generating so-called anomalous diffusion.^{5,6}

There are many scenarios where rather than analyzing the individual behavior of a single particle starting from a particular

initial condition, it is more interesting to consider the average properties of the system, taking into account an ensemble of particles. Statistical methods can then be used to describe the dynamical phenomena.^{7–9} Correspondingly, the properties and construction of the phase space can lead to what are effectively diffusion processes: as the dynamics evolves, there is diffusion of the action, usually associated with the velocity of the particles, through the phase space.

In this work, we show that the classical diffusion equation^{10–14} can be solved via a procedure well known in electrostatics, namely, the *method of images*, and used to describe the evolution of the average velocity for a system characterized by a mixed phase space. We will demonstrate the effectiveness and utility of this idea by applying it to the well-known and widely-studied Fermi-Ulam model (FUM). The results here are closely connected to a prior result shown in Ref. 15; however, in the present case, we use an approach that is part-analytical and part-empirical.

This paper is organized as follows. In Sec. II, we describe the FUM, showing the nonlinear map associated with the dynamics and introducing a picture of a diffusion process occurring within its characteristic phase space. Section III develops a theoretical framework yielding analytical results for normal diffusion in a mixed phase space. In Sec. IV, we compare these analytical results with numerical data. Conclusions are drawn in Sec. V.

II. MODEL AND PHASE SPACE

The FUM¹⁶ is a version of the Fermi accelerator, which was originally introduced by Fermi¹⁷ as a possible explanation for

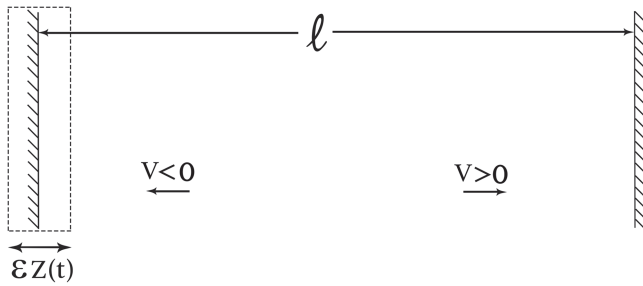


FIG. 1. Illustration of the Fermi-Ulam model. The geometrical parameter ℓ is the distance between the two walls, and the direction of the vectors denotes the sign of the particle's velocity. Usually, the time-dependent function $Z(t)$ is chosen as $\cos(\omega t)$, with ω being the frequency of oscillation.

the production of very high energy cosmic rays. Its acceleration mechanism involves the repulsion of an electrically charged particle by strong oscillatory magnetic fields, a process that is analogous to a classical particle colliding with an oscillating physical boundary. The model consists of a particle bouncing back and forth between two rigid walls, one of which is fixed, whereas the other moves periodically in time with a normalized amplitude ε , as shown schematically in Fig. 1.

The system is described by a two-dimensional, nonlinear, area-preserving map $T(V_n, \phi_n) = (V_{n+1}, \phi_{n+1})$. The velocity of the particle is the action variable and the phase, related to the time-dependent boundary, is the angle variable. Taking into account that the absolute value of the velocity changes at the moment of each collision, the mapping for the simplified version can be obtained if we approximate the oscillating wall as fixed. When the particle suffers a collision, it exchanges momentum appropriate to a moving wall. This simplified version is valid when the nonlinear parameter ε is relatively small. Hence, the simplified map of the FUM is

$$T : \begin{cases} V_{n+1} = |V_n - 2\varepsilon \sin(\phi_{n+1})|, \\ \phi_{n+1} = [\phi_n + \frac{2}{V_n}] \pmod{2\pi}. \end{cases} \quad (1)$$

The term $\frac{2}{V_n}$ corresponds to the time between collisions and $-2\varepsilon \sin(\phi_{n+1})$ gives the gain or loss of velocity/energy in each collision.

The phase space $V \times \phi$ for the FUM is composed of chaotic seas and KAM islands and is accordingly classified as a mixed phase space. In addition, it is bounded by an invariant spanning curve, which plays the role of a boundary: trajectories of lower velocity will never visit a region above this curve, no matter how many times the trajectory is iterated.

The average velocity of an ensemble of particles inside the FUM grows initially¹⁸ and then flattens off toward a plateau. This velocity growth and saturation can be interpreted as involving a diffusion process, albeit diffusion not in the physical space of the FUM, but rather in its phase space. Figure 2 shows how this phase-space diffusion behaves for different numbers of iterations n . At $n = 0$, we have the initial Gaussian-shaped distribution centered at $V_0 = 0.01$ and $\phi_0 = \pi$; then, one iteration later, the distribution seems to have become spread out uniformly along the phase axis, a fact that will

be used later in the analytic approach. However, diffusion also starts on the action axis. After 10 and then 100 iterations of the mapping [Eq. (1)], the action/velocity still continues its diffusion through the phase space. For all panels of Fig. 2, $\varepsilon = 0.001$.

It is important to bear in mind that the phase-space diffusion is limited down by null velocity and up by the first invariant spanning curve. Its position is approximated by $V_f \approx 2\sqrt{\varepsilon}$. The localization of such a curve can be obtained by using a connection with the standard mapping,^{1,19} which is written as

$$T : \begin{cases} I_{n+1} = I_n + K \sin(\theta_n), \\ \theta_{n+1} = [\theta_n + I_n], \pmod{2\pi}, \end{cases} \quad (2)$$

where the parameter K controls the intensity of the nonlinearity of the mapping. There are two transitions in the standard mapping: (i) integrability when $K = 0$ to nonintegrability for any $K \neq 0$ and (ii) a transition from local chaos when $K < K_c$ to global chaos for $K > K_c$. The parameter $K_c = 0.9716\dots$ identifies the critical value of the control parameter where all of the invariant spanning curves are destroyed, letting the dynamics diffuse unbounded in the I direction. This is exactly the transition we want to use in connection with the FUM as an attempt to describe the localization of the first invariant spanning curve. Above the curve in the FUM, one observes local chaos, an infinity of other invariant spanning curves, and eventually periodic orbits. Below the first invariant spanning curve, only chaos, periodic, and quasiperiodic dynamics coexist, each one of them being visited as determined by the initial conditions. The procedure to obtain V_f consists of describing the position of the first invariant spanning curve in the FUM through a local description of the standard mapping. Then, a Taylor expansion (see Ref. 19 for more details in a family of area preserving mappings) is made in the first equation of mapping (1) by using the fact that the invariant spanning curve is written as $V_n = V_f + \Delta V_n$, where $\Delta V_n \ll V_f$ is a small perturbation of the typical value V_f . A first order approximation leads to the expression $V_f \approx 2\sqrt{\varepsilon}$.

III. ANALYTICAL PROCEDURE

Essentially, the action variable V is undergoing a diffusion process within the bounded space $V \in [0, V_f]$. This can be described by the diffusion equation with no flux through its boundaries $\frac{\partial \rho(0,t)}{\partial V} = \frac{\partial \rho(V_f,t)}{\partial V} = 0, \forall t > 0$. Thus, the problem may be reduced to that of solving the diffusion equation to obtain the probability density function $\rho(V, t)$; once this has been integrated along the bounded space $\langle V \rangle = \int_0^{V_f} V \rho(V, t) dV$, it yields a theoretical prediction for the average velocity of $\langle V \rangle$ of particles inside the FUM.

The solution of the diffusion equation with no flux through the boundaries can be obtained analytically by the method of images, as in electrostatics.²⁰ Basically, the idea is to treat the initial Gaussian distribution as a point charge and the boundaries as conducting planes. The solution will then be an infinite sum of Gaussian functions, or normal distributions, centered at V_0 , due to the infinity of images of the initial profile. Normal distributions are characterized by their mean value $\mu \equiv \langle V \rangle$ and variance $\sigma^2 \equiv \langle V^2 \rangle - \langle V \rangle^2$. Likewise, the diffusion coefficient can be written as a function of the time derivative of the variance $D = \frac{1}{2} \frac{d\sigma^2}{dt} \rightarrow \sigma^2 = 2Dt$. The solution can then

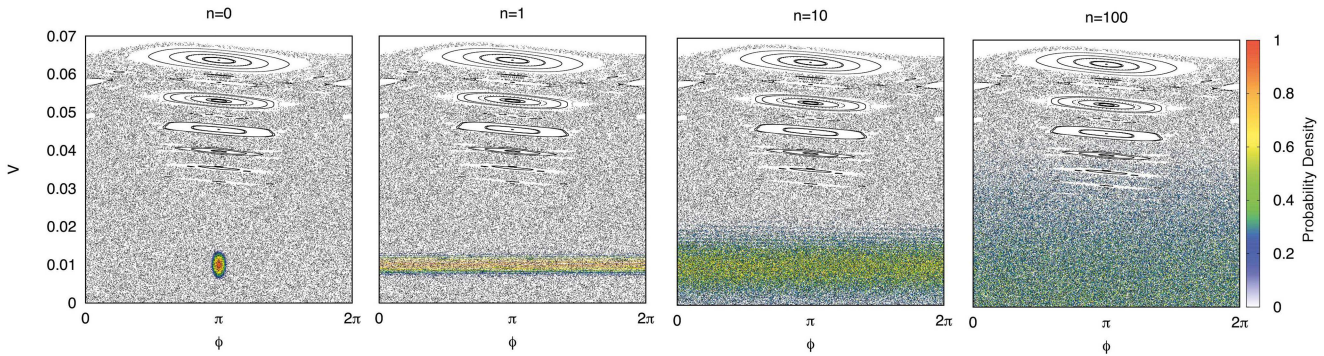


FIG. 2. Phase-space diffusion in the FUM, as sketched in Fig. 1 and described by the mapping (1). It is illustrated by the probability density in a chaotic region of the FUM's phase space, for different numbers of iterations n . The color scale shows how likely it is to find an orbit at that area of the phase space. The initial distribution, centered at $\phi_0 = \pi$, $V_0 = 0.01$ with a standard deviation $\sigma_{\phi_0} = 0.05$ and $\sigma_{V_0} = 0.001$, was plotted overlaying the phase space generated for the same parameter. As n increases, the distribution instantly spreads out uniformly along the ϕ axis and also diffuses, albeit more slowly, toward smaller and larger V .

be rewritten in terms of μ and σ^2 as

$$\rho(V; \mu, \sigma^2) = \frac{1}{\sqrt{2\pi\sigma^2}} e^{-\frac{(V-\mu)^2}{2\sigma^2}}. \quad (3)$$

Knowing the fundamental solution and applying the principle of superposition as in the method of images, we know that a sum of Gaussian functions is a solution to the problem. Hence, the solution when $V \in [0, V_f]$ with $\frac{\partial \rho(0,t)}{\partial V} = \frac{\partial \rho(V_f,t)}{\partial V} = 0$ is given by²¹

$$\rho(V; \mu, \sigma^2) = \frac{1}{\sqrt{2\pi\sigma^2}} \sum_{m=-\infty}^{\infty} \left[\exp\left(-\frac{(V - 2mV_f - \mu)^2}{2\sigma^2}\right) + \exp\left(-\frac{(V - 2mV_f + \mu)^2}{2\sigma^2}\right) \right]. \quad (4)$$

As it stands, however, this solution is not normalized for the space interval $V \in [0, V_f]$. To effect normalization, it is necessary that $A \int_0^{V_f} \rho(V; \mu, \sigma^2) dV = 1$, with A equal to a normalization constant. Considering the error function property $\text{erf}(-x) = -\text{erf}(x)$, the normalized solution is given by

$$\rho(V; \mu, \sigma^2) = \frac{1}{2A\sqrt{2\pi\sigma^2}} \sum_{m=-\infty}^{\infty} \left[\exp\left(-\frac{(V - 2mV_f - \mu)^2}{2\sigma^2}\right) + \exp\left(-\frac{(V - 2mV_f + \mu)^2}{2\sigma^2}\right) \right], \quad (5)$$

with $A = \sum_{m=-\infty}^{\infty} \text{erf}\left(\frac{\mu - 2mV_f}{\sqrt{2\sigma^2}}\right) - \text{erf}\left(\frac{\mu - V_f - 2mV_f}{\sqrt{2\sigma^2}}\right) - \text{erf}\left(\frac{\mu + 2mV_f}{\sqrt{2\sigma^2}}\right) + \text{erf}\left(\frac{\mu + V_f + 2mV_f}{\sqrt{2\sigma^2}}\right)$.

Figure 3 shows how the analytical solution for the probability density given by Eq. (5) fits the numerical simulation data for the FUM. The initial conditions for the analytic curve are the same as those used in constructing Fig. 2, with $V_0 = 0.01$, $\sigma_{V_0} = 0.001$, and $\varepsilon = 0.001$. This comparison²² provides a convincing verification of the analytical solution. The good fit indicates that the solution is suitable when considering an initial profile in a chaotic region

and neglecting the anomalous diffusion phenomena around KAM islands.

Having obtained this solution, we need to calculate the average as $\langle V \rangle = \int_0^{V_f} V \rho(V; \mu, \sigma^2) dV$ in order to be able to predict analytically the average behavior of the velocity. Because of the lack of symmetry, this calculation is nontrivial, but, integrating between the upper and lower limits using the Jacobi theta function representation,²³ we find that the solution, in terms of an important auxiliary variable $z = \frac{\mu}{\sqrt{2\sigma^2}}$ and a new parameter $\tilde{v} = \frac{V_f}{\sqrt{2\sigma^2}}$, can be written as

$$\langle V \rangle = \frac{\mu}{2A} \sum_{m=-\infty}^{\infty} \frac{1}{z\sqrt{\pi}} (\Delta^{(1)} \exp + \Delta^{(2)} \exp) + \frac{1}{\mu} \left[\left(\frac{2mV_f}{\sqrt{2\sigma^2}} - \mu \right) \Delta^{(1)} \text{erf} + \left(\frac{2mV_f}{\sqrt{2\sigma^2}} + \mu \right) \Delta^{(2)} \text{erf} \right], \quad (6)$$

with $A = \sum_{m=-\infty}^{\infty} \text{erf}\left(z - \frac{2mV_f}{\sqrt{2\sigma^2}}\right) - \text{erf}\left(z - \tilde{v} - \frac{2mV_f}{\sqrt{2\sigma^2}}\right) - \text{erf}\left(z + \frac{2mV_f}{\sqrt{2\sigma^2}}\right) + \text{erf}\left(z + \tilde{v} + \frac{2mV_f}{\sqrt{2\sigma^2}}\right)$ and

$$\begin{aligned} \Delta^{(1)} \exp &= e^{-\left(z - \frac{2mV_f}{\sqrt{2\sigma^2}}\right)^2} - e^{-\left(z - \frac{2mV_f}{\sqrt{2\sigma^2}} + \tilde{v}\right)^2}, \\ \Delta^{(2)} \exp &= e^{-\left(z + \frac{2mV_f}{\sqrt{2\sigma^2}}\right)^2} - e^{-\left(z + \frac{2mV_f}{\sqrt{2\sigma^2}} - \tilde{v}\right)^2}, \\ \Delta^{(1)} \text{erf} &= \text{erf}\left(z - \frac{2mV_f}{\sqrt{2\sigma^2}} + \tilde{v}\right) - \text{erf}\left(z - \frac{2mV_f}{\sqrt{2\sigma^2}}\right), \\ \Delta^{(2)} \text{erf} &= \text{erf}\left(z + \frac{2mV_f}{\sqrt{2\sigma^2}}\right) - \text{erf}\left(z + \frac{2mV_f}{\sqrt{2\sigma^2}} + \tilde{v}\right). \end{aligned}$$

Furthermore, the mean μ and variance σ^2 are calculated, by construction, over the point charge, which is characterized by an unbounded diffusion process. According to our initial mapping, Eq. (1), the point charge mapping is given by $V_{n+1} = V_n - 2\varepsilon \sin(\phi)$, where ϕ is a uniform random variable; as observed in Fig. 2, it is then

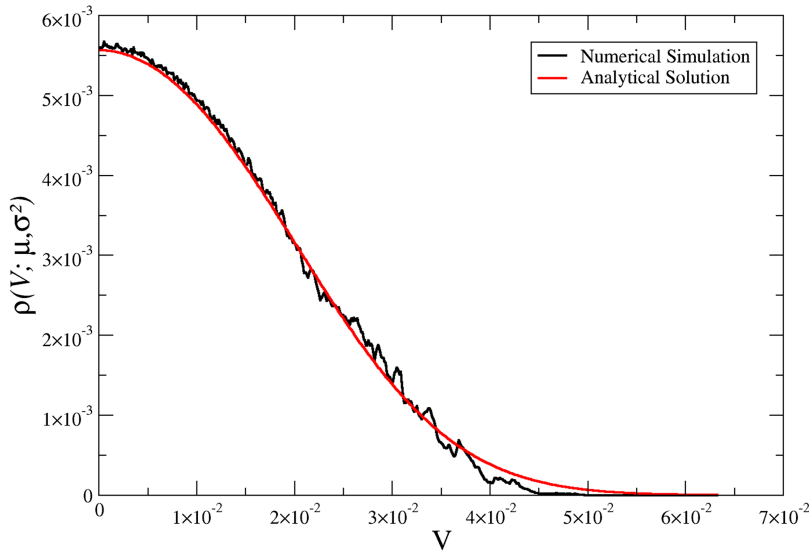


FIG. 3. Comparison between the analytical solution and the experimental/numerical probability distribution of the diffusion process depicted in Fig. 2. This is the behavior after 100 iterations.

possible to write the mean and variance for the point charge as

$$\begin{aligned} \mu_{n+1} &= \langle V_{n+1} \rangle = \langle V_n \rangle \Rightarrow \mu = \mu_0 = V_0, \\ \sigma_{n+1}^2 &= \langle V_{n+1}^2 \rangle - \langle V_{n+1} \rangle^2 = \langle V_n^2 \rangle + 2\varepsilon^2 - \langle V_n \rangle^2 \\ &\Rightarrow \sigma_{n+1}^2 = \sigma_n^2 + 2\varepsilon^2. \end{aligned}$$

Following the theory of difference equations,²⁴ assuming a large number of iterations and small values of ε , it is then possible to write σ as a function of n ,

$$\sigma_{n+1}^2 - \sigma_n^2 = \frac{d\sigma^2}{dn} \Rightarrow \sigma^2(n) = \sigma_0^2 + 2\varepsilon^2 n. \quad (7)$$

This result is important because it carries the information that the variance is a function of the number of iterations $\sigma^2 = \sigma^2(n)$, connecting the solution of the diffusion equation to the discrete mapping of the FUM. Moreover, the initial variance σ_0 is zero if the initial profile is considered a perfect Dirac delta function. This also tells us that the diffusion is normal, since $\sigma \propto \sqrt{n}$. In addition, it is also possible to calculate the diffusion coefficient, which is a constant and quite intuitive with our suppositions for this case so that $D = \varepsilon^2$. Then, z is also a function of the number of iterations n such that

$$z = \frac{\mu}{\sqrt{2\sigma(n)}} \Rightarrow z(n) = \frac{V_0}{2\varepsilon\sqrt{n}}. \quad (8)$$

Substituting Eq. (8) into Eq. (6), we can calculate how the average velocity behaves as a function of the number of iterations for the dynamics of the FUM. However, of course, we now need to check whether, or not, this theory really describes the actual behavior of the average velocity.

IV. ANALYTICAL x NUMERICAL RESULTS

Figure 4 compares the numerical simulation data with the analytic predictions of Eqs. (6) and (8). The expression for $\langle V \rangle$, given by Eq. (6), represents a continuous competition between the exponential and error functions, so it is interesting to study their arguments.

Based on a graphical analysis, we conclude that there are two changes of behavior: at $z = 1$ and at $\tilde{v} = 1$. First, taking $z = 1$,

$$z = 1 \Rightarrow \frac{V_0}{2\varepsilon\sqrt{n}} = 1 \Rightarrow n = \left(\frac{V_0}{2\varepsilon}\right)^2 \Rightarrow n = \frac{V_0^2}{4\varepsilon^2},$$

but in this case, $n = n_x$ marking the first crossover.²⁵ Thus,

$$n_x = \frac{V_0^2}{4\varepsilon^2}. \quad (9)$$

Second, taking $\tilde{v} = 1$,

$$\tilde{v} = 1 \Rightarrow \frac{V_f}{2\varepsilon\sqrt{n}} = 1 \Rightarrow n \approx \left(\frac{2\sqrt{\varepsilon}}{2\varepsilon}\right)^2 \Rightarrow n \approx \frac{1}{\varepsilon},$$

but now, $n = n'_x$ marking the second crossover. Thus,

$$n'_x \approx \frac{1}{\varepsilon}. \quad (10)$$

Another important result is the limit,

$$\lim_{\sigma \rightarrow \infty} \langle V \rangle = \lim_{n \rightarrow \infty} \langle V \rangle = \frac{V_f}{2} \approx \sqrt{\varepsilon}, \quad (11)$$

which provides the saturation value V_{sat} . Then, Fig. 4 shows the average velocity for an ensemble of 10^3 particles, all with initial velocity $V_0 = 2 \times 10^{-3}$, taken within the interval $\phi_0 \in [0, 2\pi]$. The analytical predictions for the first crossover n_x , Eq. (9); the second crossover n'_x , Eq. (10); and the saturation plateau when $n \rightarrow \infty$, Eq. (11), are shown by the dashed lines.

The analytical approach, yielding Eq. (6), clearly agrees well with the numerical simulation data. The correspondence might have been even closer if it were not for the fact that the diffusion is not normal for higher values of V , due to the effect of the islands in this region of the phase space. This also explains the fluctuation for $n > n'_x$. The diffusion around stability structures such as KAM islands leads to the very complicated behavior known as anomalous diffusion. However, the associated stickiness of the dynamics near the islands, though

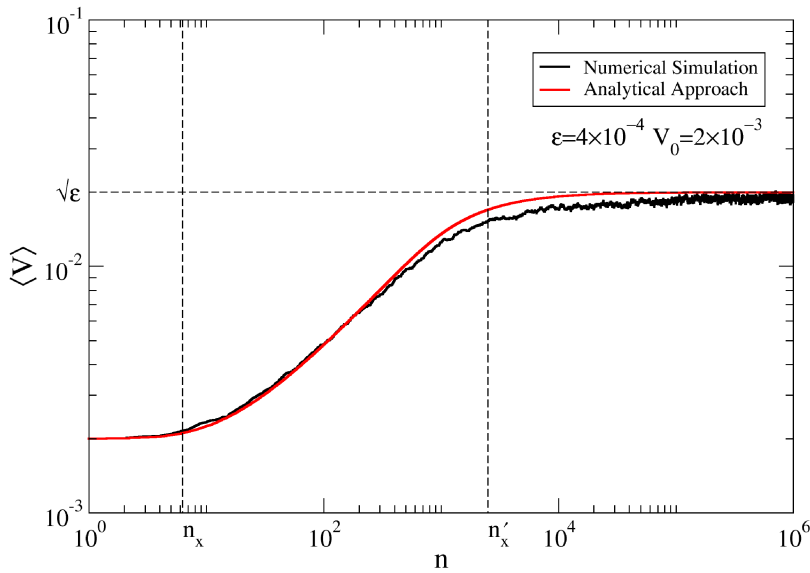


FIG. 4. The average velocity $\langle V \rangle$ of particles in the FUM showing its evolution with the number of iterations n . With parameter $\epsilon = 4 \times 10^{-4}$, an ensemble of 10^3 particles, each with $V_0 = 2 \times 10^{-3}$, was iterated until there had been 10^6 collisions. The numerical simulations (rough black line) are compared with the analytic theory (smooth red line). Note the saturation of $\langle V \rangle$ toward $\sqrt{\epsilon}$ that occurs at large n in both theory and simulation. The discrepancies are due to the effect of anomalous diffusion around KAM islands.

real, is a relatively minor effect given the size of the whole phase space: Harsoula *et al.*²⁶ conclude that, for a long enough interval, averaging over the ensemble smoothes the observables so that the stickiness can largely be neglected.

Figure 5 compares numerical data with the corresponding analytical predictions for three different initial velocities V_0 and values of the control parameter ϵ . It is important to remember that the position of the upper boundary in the phase space, which is the first invariant spanning curve, is approximated by $V_f \approx 2\sqrt{\epsilon}$. Then, for each value of the parameter ϵ , a different bounded phase space is considered. Again, it is evident that the analytic curves provide an excellent fit to the numerical data, even for relatively large values of ϵ .

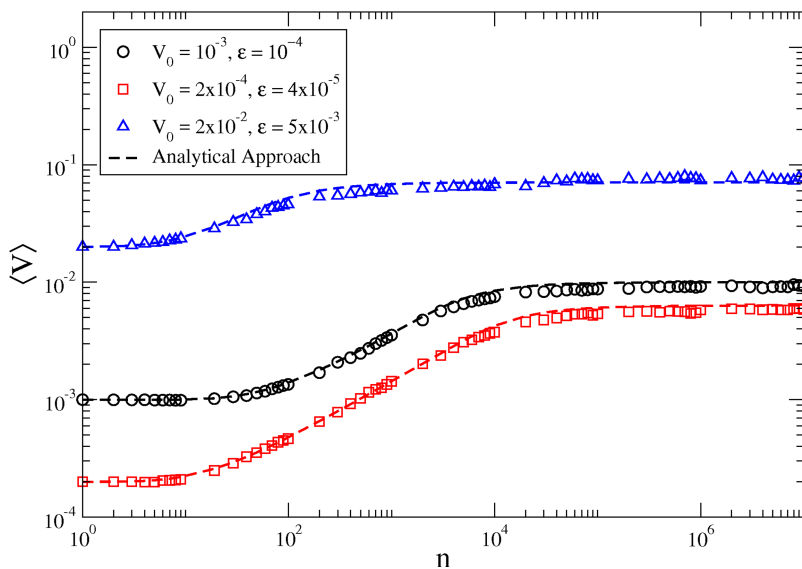


FIG. 5. The average velocity $\langle V \rangle$ of particles in the FUM showing how it evolves with the number of iterations n , under different conditions. The analytic theory (dashed lines) is compared with numerical simulations (data points) for three different initial velocities V_0 and values of the control parameter ϵ , as listed in the inset. In each case, the simulations involved an ensemble of 10^4 particles iterated up to 10^7 collisions.

We emphasize that Eqs. (9)–(11) represent the first analytic predictions to be made for the Fermi-Ulam model. They agree well with what was proposed on purely empirical grounds¹⁵ more than a decade ago. Three hypotheses were then proposed, based on a scaling analysis: (i) $n_x \propto \frac{V_0^2}{\epsilon^2}$, which agrees perfectly with Eq. (9), and we now also obtain the proportionality constant $\frac{1}{4}$; in addition, (ii) $n'_x \propto \frac{1}{\epsilon}$, which agrees with Eq. (10); and finally, (iii) $V_{sat} \propto \epsilon^\alpha$, with $\alpha \approx \frac{1}{2}$, which agrees with Eq. (11).

V. CONCLUSION

We conclude that a combination of the theory of diffusive processes with dynamical systems theory, plus the method of images

from electrostatics, provides a different method for treating systems described by nonlinear mappings. The method can be expected to work for mixed phase spaces that are delimited by boundaries through which there are no fluxes. Application to the Fermi-Ulam model, taken as an example, has yielded some interesting features and good agreement both with numerical simulations and with earlier empirically-based theoretical considerations. We expect that, for larger values of the control parameter, the results would not hold because the effect of the islands and, therefore, of anomalous diffusion could not then be neglected. Extension of the procedure discussed here to time-dependent billiards²⁷ is an interesting possibility for future work.

ACKNOWLEDGMENTS

We gratefully acknowledge valuable discussions with Professor Roberto Lagos. M. S. Palmero was supported by Fundação de Amparo à Pesquisa do Estado de São Paulo (FAPESP) from Brazil (Process Nos. 2014/27260-5 and 2016/15713-0). G. I. Díaz acknowledges the Brazilian agency CNPq. This research was supported by the Engineering and Physical Sciences Research Council (United Kingdom) [EPSRC(GB)] under Grant Nos. GR/R03631 and EP/M015831/1. E. D. Leonel acknowledges support from CNPq (No. 303707/2015-1) and FAPESP (No. 2017/14414-2).

REFERENCES

- ¹A. J. Lichtenberg and M. A. Leiberman, *Regular and Chaotic Dynamics* (Springer, Berlin, 1992).
- ²E. Ott, "Goodness of ergodic adiabatic invariants," *Phys. Rev. Lett.* **42**, 1628–1631 (1979).
- ³B. V. Chirikov, "A universal instability of many-dimensional oscillator systems," *Phys. Rep.* **52**, 263–379 (1979).
- ⁴R. Venegeroles, "Calculation of superdiffusion for the Chirikov-Taylor model," *Phys. Rev. Lett.* **101**, 054102 (2008).
- ⁵G. M. Zaslavsky, *Physics of Chaos in Hamiltonian Systems* (Imperial College Press, London, 2007).
- ⁶J. Klafter and I. M. Sokolov, "Anomalous diffusion spreads its wings," *Phys. World* **18**, 29–32 (2005).
- ⁷R. Venegeroles, "Universality of algebraic laws in Hamiltonian systems," *Phys. Rev. Lett.* **102**, 064101 (2009).
- ⁸O. Alus, S. Fishman, and J. D. Meiss, "Universal exponent for transport in mixed Hamiltonian dynamics," *Phys. Rev. E* **96**, 032204 (2017).
- ⁹R. M. da Silva, M. W. Beims, and C. Manchein, "Recurrence-time statistics in non-Hamiltonian volume-preserving maps and flows," *Phys. Rev. E* **92**, 022921 (2015).
- ¹⁰P. J. Basser and D. K. Jones, "Diffusion-tensor MRI: Theory, experimental design and data analysis—A technical review," *NMR Biomed.* **15**, 456–467 (2002).
- ¹¹H. A. Kramers, "Brownian motion in a field of force and the diffusion model of chemical reactions," *Physica* **7**, 284–304 (1940).
- ¹²J. D. Meiss, "Thirty years of turnstiles and transport," *Chaos* **25**, 097602 (2015).
- ¹³E. G. Altmann, J. S. E. Portela, and T. Tél, "Leaking chaotic systems," *Rev. Mod. Phys.* **85**, 869–918 (2013).
- ¹⁴G. M. Zaslavsky, "Chaos, fractional kinetics, and anomalous transport," *Phys. Rep.* **371**, 461–580 (2002).
- ¹⁵E. D. Leonel, P. V. E. McClintock, and J. K. L. da Silva, "Fermi-Ulam accelerator model under scaling analysis," *Phys. Rev. Lett.* **93**, 014101 (2004).
- ¹⁶M. A. Lieberman and A. J. Lichtenberg, "Stochastic and adiabatic behavior of particles accelerated by periodic forces," *Phys. Rev. A* **5**, 1852–1866 (1971).
- ¹⁷E. Fermi, "On the origin of the cosmic radiation," *Phys. Rev.* **75**, 1169–1174 (1949).
- ¹⁸T. Pereira and D. Turaev, "Exponential energy growth in adiabatically changing Hamiltonian systems," *Phys. Rev. E* **91**, 010901 (2015).
- ¹⁹E. D. Leonel, J. A. de Oliveira, and F. Saif, "Critical exponents for a transition from integrability to non-integrability via localization of invariant tori in the Hamiltonian system," *J. Phys. A* **44**, 302001 (2011).
- ²⁰J. Crank, *The Mathematics of Diffusion* (OUP, Oxford, 1975).
- ²¹R. N. Bhattacharya and E. C. Waymire, *Stochastic Processes with Applications* (SIAM, 2009).
- ²²C. Lozej and M. Robnik, "Aspects of diffusion in the stadium billiard," *Phys. Rev. E* **97**, 012206 (2018).
- ²³J. M. Borwein and P. B. Borwein, *Pi and the AGM: A Study in Analytic Number Theory and Computational Complexity* (Wiley, Toronto, 1987).
- ²⁴C. M. Bender and S. A. Orszag, *Advanced Mathematical Methods for Scientists and Engineers I: Asymptotic Methods and Perturbation Theory* (Springer, Berlin, 1999).
- ²⁵The crossover number is defined as the iteration number that marks some dynamical change, for example, the change from growth to saturation.
- ²⁶M. Harsoula, K. Karamanos, and G. Contopoulos, "Characteristic times in the standard map," *Phys. Rev. E* **99**, 032203 (2019).
- ²⁷K. Shah, V. Gelfreich, V. Rom-Kedar, and D. Turaev, "Leaky Fermi accelerators," *Phys. Rev. E* **91**, 062920 (2015).